



ELSEVIER

Available at  
**WWW.MATHEMATICSWEB.ORG**  
POWERED BY SCIENCE @ DIRECT®

Applied Numerical Mathematics 45 (2003) 331–351



**APPLIED  
NUMERICAL  
MATHEMATICS**

[www.elsevier.com/locate/apnum](http://www.elsevier.com/locate/apnum)

# ADI schemes for higher-order nonlinear diffusion equations

T.P. Witelski <sup>a,\*</sup>, M. Bowen <sup>b</sup>

<sup>a</sup> *Department of Mathematics and the Center for Nonlinear and Complex Systems, Duke University,  
Durham, NC 27708-0320, USA*

<sup>b</sup> *School of Mathematical Sciences, University of Nottingham, University Park, Nottingham, NG7 2RD, UK*

---

## Abstract

Alternating Direction Implicit (ADI) schemes are constructed for the solution of two-dimensional higher-order linear and nonlinear diffusion equations, particularly including the fourth-order thin film equation for surface tension driven fluid flows. First and second-order accurate schemes are derived via approximate factorization of the evolution equations. This approach is combined with iterative methods to solve nonlinear problems. Problems in the fluid dynamics of thin films are solved to demonstrate the effectiveness of the ADI schemes.

© 2002 IMACS. Published by Elsevier Science B.V. All rights reserved.

*Keywords:* ADI methods; Nonlinear diffusion equations; Parabolic PDE; Approximate factorization; Higher-order equations

---

## 1. Introduction

In this article we build on the existing literature for second-order problems to construct and compare classes of alternating direction implicit (ADI) schemes for nonlinear higher-order parabolic equations. For nonlinear problems, we combine this approach with iterative methods for solving nonlinear systems [39,58]. As in [36], we focus on the time-stepping of the ADI schemes, and expect that the effects of spatial discretization in the numerical simulations will not significantly change our analysis of smooth solutions for diffusive problems. We present these schemes in terms of approximate factorization of the evolution equation [26,44,64] although they may also be interpreted in terms of additive operator splitting [35,44].

Use of ADI methods for linear second- and fourth-order parabolic problems has a long history [14,24]. Recent work in numerical simulations of problems in fluid dynamics [28,29,59,60], has made extensive use of these classical methods [14–16]. We extend this foundation and focus on the solution of fourth-

---

\* Corresponding author.

*E-mail addresses:* [witelski@math.duke.edu](mailto:witelski@math.duke.edu) (T.P. Witelski), [mark.bowen@nottingham.ac.uk](mailto:mark.bowen@nottingham.ac.uk) (M. Bowen).

order nonlinear parabolic equations in two dimensions. These problems arise in the study of surface tension driven flow of thin liquid films [50,55]. In the formulation of these free surface problems, the local flux of fluid is determined by gradients of the curvature of the surface. Such evolution equations for the motion of the graph of the free surface  $z = u(x, y, t)$  take the general form,

$$\frac{\partial u}{\partial t} + \nabla \cdot (f(u)\nabla H) = 0, \quad (1.1)$$

where  $H$  is the mean curvature of the surface. In the study of lubrication flows of thin liquid films, the mean curvature of the surface [22] is approximated by the Laplacian in the small gradient limit,  $|\nabla u| \ll 1$ ,

$$H = \frac{u_{xx}\sqrt{1+u_y^2} + u_{yy}\sqrt{1+u_x^2} - 2u_xu_yu_{xy}}{(1+u_x^2+u_y^2)^{3/2}} = u_{xx} + u_{yy} + O(|\nabla u|^2), \quad (1.2)$$

to yield a class of fourth-order nonlinear diffusion equations, called generalized thin film equations [9, 50,55],

$$\frac{\partial u}{\partial t} + \nabla \cdot (f(u)\nabla\nabla^2 u) = 0. \quad (1.3)$$

A brief list of some recent research in fluid dynamics involving numerical simulations of this class of two-dimensional problem includes [21,28,29,52,53,59,60]. For most of this article we will focus on methods for the thin film equation (1.3), however we will also describe how our methods can naturally be applied to more strongly nonlinear equations like (1.1). Generalizations of (1.1), where  $f$  also depends on gradients of  $u$ , have also been applied to problems involving surface diffusion of thin solid films [8], generalized curvature evolution models for image processing [63,65], flows of non-Newtonian fluids [42], and many other models in emerging areas of scientific research [41].

The numerical solution of differential equations of the form (1.3) poses several problems;

- (i) fourth-order parabolic equations are very stiff; the stability constraint on the time-step for explicit methods,  $\Delta t = O(\Delta x^4)$ , is prohibitive, hence implicit methods are necessary,
- (ii) Eq. (1.3) is quasilinear and (1.1) is strongly nonlinear, hence convergence and accuracy are important considerations,
- (iii) for fluid dynamics applications, (1.3) is a degenerate equation, with  $f(u) = O(u^p)$  as  $u \rightarrow 0$  with  $p \geq 0$ , numerical solution of problems of this form become very sensitive to details of the numerical scheme for  $u \rightarrow 0$  [9,33,67],
- (iv) for two-dimensional problems, the spatial operator necessarily includes mixed derivative terms which complicate splitting schemes.

The ADI schemes developed in this paper take a form that is easily generalized to the higher-order analogue of (1.3) [7,41,61],

$$\frac{\partial u}{\partial t} + (-1)^{m-1}\nabla \cdot (f(u)\nabla\nabla^{2m}u) = 0, \quad m = 2, 3, \dots \quad (1.4)$$

These yet-higher-order equations have been suggested in connection with diffusion in semi-conductors and in other physical systems [41]. Very little work has been done on these models, partly because they accentuate the difficulties of (1.3)—they are even stiffer and have many more mixed derivative terms. However, we will show that they can be treated in the same framework as (1.3) with our ADI schemes.

In Section 2 we investigate linear constant coefficient problems for (1.3) and (1.4) with  $f(u) \equiv 1$  and further generalize these results to the case where  $f$  is a known function of  $x$ ,  $y$  and  $t$ . Section 3 addresses the nonlinear problem and discusses appropriate iterative schemes. Following this, in Section 4, we discuss discretizations of the spatial operators and relevant boundary conditions. We conclude in Section 5 by employing the ADI methods developed in the previous sections to solve problems arising out of the study of thin film flow [10,11,66].

It is hoped that this paper serves a dual role, firstly as a review of previous research on ADI schemes, and secondly to develop extensions of such schemes that can facilitate numerical studies of higher-order nonlinear parabolic problems arising from new mathematical models of a diverse range of physical phenomena [41].

## 2. The constant-coefficient linear problem

We begin with the analysis of the linear problem for (1.3) where  $f(u) \equiv 1$ ,

$$u_t + \nabla^4 u = 0, \quad (2.1)$$

with the two-dimensional biharmonic operator,  $\nabla^4 u \equiv u_{xxxx} + 2u_{xxyy} + u_{yyyy}$ . Equations of this form are fundamental parts of many applied mathematical models, examples of which include; the Cahn–Hilliard equation for binary mixtures [27,51], the Kuramoto–Sivashinsky equation for instabilities of flame fronts in combustion theory [37], the Benney equation for surface waves on liquid films [6], and linearized models of the spreading of thin viscous films [9]. ADI methods for problems involving the biharmonic operator date back to the work of Conte and Dames [14–16] describing vibrational modes for thin plates; Eq. (2.1) describes the motion of a strongly damped plate.

### 2.1. First-order methods: $\theta$ -weighted schemes

We first consider single-step time discretizations of (2.1) involving only the time-steps  $u^n$  and  $u^{n+1}$ . In this semi-discrete formulation we use the notation  $u(x, y, t^n) = u^n(x, y)$  and  $t^{n+1} = t^n + \Delta t$ , where the superscripts denote discrete time steps. The finite difference approximation of the time derivative is taken to be  $u_t = (u^{n+1} - u^n)/\Delta t + O(\Delta t)$ . We apply the spatial operator to  $u = \theta u^{n+1} + (1 - \theta)u^n$ , called the one-step generalized trapezoid rule or  $\theta$ -weighted scheme. The discretization for (2.1) is then given by

$$u^{n+1} - u^n + \Delta t [\theta \nabla^4 u^{n+1} + (1 - \theta) \nabla^4 u^n] = 0. \quad (2.2)$$

For  $\theta = 1/2$ , (2.2) is a second-order accurate Crank–Nicolson scheme; for all other  $\theta$  in  $0 \leq \theta \leq 1$ , the scheme is first-order accurate. For  $\theta = 0$ , (2.2) yields an explicit forward Euler scheme, while  $\theta = 1$  corresponds to the unconditionally stable backward Euler method. Solving (2.2) for any  $\theta \neq 0$  is an implicit problem for  $u^{n+1}$  involving the inversion of a two-dimensional spatial operator. Using approximate factorization of this operator, ADI schemes solve this problem through the inversion of simpler one-dimensional operators.

Separating implicit and explicit terms in (2.2) yields

$$(\mathbf{I} + \theta \Delta t \nabla^4) u^{n+1} = (\mathbf{I} - (1 - \theta) \Delta t \nabla^4) u^n, \quad (2.3)$$

where  $I$  is the identity operator. The two-dimensional spatial operator acting on  $u^{n+1}$  in (2.3) can be expressed a sum of mixed-derivative terms and products of one-dimensional operators,

$$I + \theta \Delta t \nabla^4 = L_x L_y + 2\theta \Delta t \partial_{xxyy} - \theta^2 \Delta t^2 D_x D_y, \quad (2.4)$$

where the one-dimensional operators used above are

$$L_x = I + \theta \Delta t D_x, \quad L_y = I + \theta \Delta t D_y, \quad (2.5)$$

with

$$D_x = \partial_{xxxx}, \quad D_y = \partial_{yyyy}. \quad (2.6)$$

Since (2.3) is at most second-order accurate, without loss of accuracy we can apply the  $O(\Delta t^2)$  eighth derivative operator, the last term on the right-side of (2.4), to  $u^n$  instead of  $u^{n+1}$  to reduce it to an explicit term while introducing only higher-order corrections,  $O(\Delta t^3)$ . Applying the same approximation to the mixed-derivative term  $2\theta \Delta t \partial_{xxyy}$  similarly shifts it to operate on the explicit solution  $u^n$ , at the price of reducing the scheme to first-order accuracy in time for all  $\theta$ ,

$$L_x L_y u^{n+1} = (I - (1 - \theta) \Delta t \nabla^4 - 2\theta \Delta t \partial_{xxyy} + \theta^2 \Delta t^2 D_x D_y) u^n. \quad (2.7)$$

If the mixed derivative were not present, then second-order accuracy in time could be achieved for  $\theta = 1/2$ . ADI schemes for second-order linear parabolic equations with mixed derivative terms have been considered by many authors [5,17,23,45,46,48]. Beam and Warming [5] give a thorough analysis of linear one- and two-step ADI methods for second-order linear parabolic equations and show that the restriction to first-order accuracy for one-step methods is unavoidable in the presence of mixed derivatives.

We note that Douglas and Gunn [23] suggested a splitting scheme using four operators allowing mixed derivative terms to be treated implicitly, however their approach cannot easily be extended to the class of boundary value problems for (1.3) we seek to solve (see Section 5). We will also not pursue the option of splitting (2.1) into a system [30] of the form  $u_t = \nabla^2 P$ , with  $P = -\nabla^2 u$ , corresponding to a pressure field, though this approach has been used by other authors [3,33].

We use the approximate factorization (2.7) to write a first-order ADI scheme for (2.3) in the form

$$\begin{aligned} L_x u^* &= (I - (1 - \theta) \Delta t \nabla^4 - 2\theta \Delta t \partial_{xx} \partial_{yy}) u^n - \theta \Delta t D_y u^n, \\ L_y u^{n+1} &= u^* + \theta \Delta t D_y u^n, \end{aligned} \quad (2.8)$$

where  $u^*$  represents an intermediate result obtained from solving the  $L_x$ -problem. The original form of (2.7) can be recovered by simply applying the  $L_x$  operator to the  $L_y u^{n+1}$  equation. Eq. (2.7) can be factored to yield various ADI schemes. We do not discuss these further, however it is noteworthy that (2.8) is similar to the D'Yakanov form [47,62].

We can derive a more compact form of the ADI scheme (2.8) by subtracting  $L_x L_y u^n$  from both sides of (2.7) to yield a factored equation for the change between successive time-steps,  $v = u^{n+1} - u^n$ , [2,4,64], whereby we obtain

$$L_x L_y v = -\Delta t \nabla^4 u^n, \quad (2.9)$$

with the generalized ADI operator-split form [44,56],

$$\begin{aligned} L_x w &= -\Delta t \nabla^4 u^n, \\ (L_1) \quad L_y v &= w, \\ u^{n+1} &= u^n + v. \end{aligned} \quad (2.10)$$

We will refer to this numerical scheme as  $(L_1)$ , denoting a first-order linear-equation scheme; similar abbreviations will be used throughout.

We address the stability of the scheme (2.8) in terms of von Neumann stability analysis. Solutions of the semi-discrete model can be expressed in terms of a superposition of Fourier modes with coefficients that grow like powers of wavenumber-dependent amplification factors,  $\sigma(\mathbf{k})$ ,

$$u^n(x, y) = \sigma(\mathbf{k})^n e^{i(k_x x + k_y y)}, \tag{2.11}$$

where the superscript  $n$  in  $u^n$  denotes the time-step and the superscript on the right-side of (2.11) denotes a power of  $\sigma$ . Substituting (2.11) into (2.9) at the rescaled wavenumber,  $\hat{\mathbf{k}} = \mathbf{k}/\Delta t^{1/4}$ , yields a  $\Delta t$ -independent formula for the amplification factor for each Fourier component,

$$\sigma(\hat{\mathbf{k}}) - 1 = -\frac{(k_x^2 + k_y^2)^2}{(1 + \theta k_x^4)(1 + \theta k_y^4)}. \tag{2.12}$$

Since the right-side of (2.12) is negative definite, the requirement for unconditional stability, and hence convergence of (2.10),  $|\sigma| \leq 1$  for all  $\mathbf{k}$ , is that the fraction is less than two in magnitude. The maximum of this fraction,  $1/\theta$ , is achieved on the curve  $k_x^2 k_y^2 = 1/\theta$ . Consequently, the ADI scheme  $(L_1)$  is unconditionally stable for  $\theta \geq 1/2$ . For  $\theta < 1/2$ , Eq. (2.12) can be used to obtain the condition for stability,  $\Delta t < \Delta x^4(1 - \theta - \sqrt{1 - 2\theta})/\theta^2$ .

### 2.2. A second-order BDF method

To produce accurate calculations of long-time evolution of (2.1) it is necessary to derive numerical methods that have higher-orders of accuracy in time. To achieve second-order accuracy greater care must be taken in the approximate factorization of the implicit spatial operator, (2.7). Since, as described above, single-step ADI schemes for (2.1) can not achieve second-order accuracy [5], we turn to a two-step method. We consider a fully implicit scheme for the PDE (2.1) evaluated at time  $t^{n+1}$  and approximate the time derivative by the second-order backward differentiation formula,

$$\left. \frac{\partial u}{\partial t} \right|_{t^{n+1}} = \frac{3u^{n+1} - 4u^n + u^{n-1}}{2\Delta t} + O(\Delta t^2). \tag{2.13}$$

This discretization is a desirable choice since it yields  $A$ -stable multi-step methods [38]. Substituting this approximation into (2.1) yields

$$\left( \mathbf{I} + \frac{2}{3}\Delta t \nabla^4 \right) u^{n+1} = \frac{4}{3}u^n - \frac{1}{3}u^{n-1}, \tag{2.14}$$

with a truncation error of  $O(\Delta t^3)$ . As in (2.4), factoring the two-dimensional spatial operator acting on  $u^{n+1}$  yields a product of one-dimensional operators and mixed derivative remainders,

$$\mathbf{I} + \frac{2}{3}\Delta t \nabla^4 = \mathbf{L}_x \mathbf{L}_y + \frac{4}{3}\Delta t \partial_{xxyy} - \frac{4}{9}\Delta t^2 \mathbf{D}_x \mathbf{D}_y \tag{2.15}$$

where the one-dimensional operators  $\mathbf{L}_x, \mathbf{L}_y$  correspond to (2.5) with  $\theta = 2/3$ . As before, we can replace the  $O(\Delta t^2)$  eighth order operator by an explicit term acting on  $u^n$  without introducing any error terms below  $O(\Delta t^3)$ . However, this approximation can not be used for the mixed derivative term  $\frac{4}{3}\Delta t \partial_{xxyy} u^{n+1}$

without introducing  $O(\Delta t^2)$  errors. To avoid this difficulty, we make use of a linear extrapolation formula to derive a second-order accurate explicit approximation for  $u^{n+1}$  [5],

$$\bar{u}^{n+1} \equiv 2u^n - u^{n-1} = u^{n+1} + O(\Delta t^2). \quad (2.16)$$

The fourth-order mixed derivative term in (2.15) can then be applied to  $\bar{u}^{n+1}$ , instead of  $u^{n+1}$ , while only introducing  $O(\Delta t^3)$  errors. The resulting approximate factorization is

$$\mathbf{L}_x \mathbf{L}_y u^{n+1} = \frac{1}{3}(4u^n - u^{n-1}) - \frac{4}{3}\Delta t \partial_{xxyy} \bar{u}^{n+1} + \left(\frac{2}{3}\Delta t\right)^2 \mathbf{D}_x \mathbf{D}_y \bar{u}^{n+1}. \quad (2.17)$$

Finally, subtracting  $\mathbf{L}_x \mathbf{L}_y \bar{u}^{n+1}$  from both sides of (2.17) yields

$$\mathbf{L}_x \mathbf{L}_y v = -\frac{2}{3}(u^n - u^{n-1}) - \frac{2}{3}\Delta t \nabla^4 \bar{u}^{n+1}, \quad (2.18)$$

with  $v = u^{n+1} - \bar{u}^{n+1}$ . Consequently the ADI split form is given by

$$\begin{aligned} \mathbf{L}_x w &= -\frac{2}{3}(u^n - u^{n-1}) - \frac{2}{3}\Delta t \nabla^4 \bar{u}^{n+1}, \\ (L_2) \quad \mathbf{L}_y v &= w, \\ u^{n+1} &= \bar{u}^{n+1} + v. \end{aligned} \quad (2.19)$$

Von Neumann stability analysis of  $(L_2)$  yields the equation for the amplification factor,  $\sigma = \sigma(\hat{\mathbf{k}})$ ,

$$\left(1 + \frac{2}{3}k_x^4\right)\left(1 + \frac{2}{3}k_y^4\right)(\sigma - 1)^2 = -\frac{2}{3}(\sigma - 1) - \frac{2}{3}(k_x^2 + k_y^2)^2(2\sigma - 1). \quad (2.20)$$

This equation can be most conveniently written as a quadratic equation for  $(\sigma - 1)$ . Thereafter, direct calculation shows that both roots are in the range  $0 \leq |\sigma| \leq 1$  for all  $\mathbf{k}$ , and consequently the  $(L_2)$  scheme is unconditionally stable.

We note that  $(L_2)$  is one of a large class of second-order linear multi-step methods; we will not pursue a full analysis of the class of methods like that given by Beam and Warming [5]. However, we briefly mention another second-order scheme given by Augenbaum et al. [2] to compare its form. Originally studied in connection with a system of hyperbolic conservation laws, their scheme is derived from a Crank–Nicolson scheme, (2.3) with  $\theta = 1/2$ , which, when applied to (2.1) takes the form

$$\left(1 + \frac{1}{2}\Delta t \nabla^4\right)(u^{n+1} - u^n) = -\Delta t \nabla^4 u^n. \quad (2.21)$$

The spatial operator on the left is then expressed in terms of its approximate factorization (2.4) with  $u^{n+1}$  replaced by (2.16) in the non-factored terms without loss of second-order accuracy to yield

$$\mathbf{L}_x \mathbf{L}_y (u^{n+1} - u^n) = -\Delta t \nabla^4 u^n - \Delta t \partial_{xxyy} (\bar{u}^{n+1} - u^n) + \frac{1}{4}\Delta t^2 \mathbf{D}_x \mathbf{D}_y (\bar{u}^{n+1} - u^n). \quad (2.22)$$

We note that subtracting  $\mathbf{L}_x \mathbf{L}_y (\bar{u}^{n+1} - u^n)$  from both sides of (2.22) yields a two-step linear method of the same general form as (2.18), the  $(L_2)$  scheme. In [2] this scheme was called *the iterative reduction of factorization error procedure* and was claimed to eliminate grid-orientation errors in ADI methods.

### 2.3. Higher-order linear parabolic problems

A benefit of the of the factored forms of the ADI schemes ( $L_1$ ) and ( $L_2$ ) is that they are easily extendable to higher-order diffusion equations of the form [7,41,61]

$$u_t + (-1)^{m-1} \nabla^{2m+2} u = 0, \quad m = 1, 2, \dots, \tag{2.23}$$

where  $\nabla^{2m+2} = (\partial_{xx} + \partial_{yy})^{m+1}$ . If we define  $\mathbf{D}_x = \partial_x^{2m+2}$  and similarly for  $\mathbf{D}_y$ , then the ( $L_1$ )  $\theta$ -weighted scheme generalizes in a straightforward manner for (2.23) as

$$\begin{aligned} L_x w &= (-1)^m \Delta t \nabla^{2m+2} u^n, \\ (hL_1) \quad L_y v &= w, \\ u^{n+1} &= u^n + v. \end{aligned} \tag{2.24}$$

Von Neumann stability analysis of this scheme yields the amplification factor

$$\sigma(\hat{\mathbf{k}}) - 1 = - \frac{(k_x^2 + k_y^2)^{m+1}}{(1 + \theta k_x^{2m+2})(1 + \theta k_y^{2m+2})}, \tag{2.25}$$

where  $\hat{\mathbf{k}} = \mathbf{k} / \Delta t^{1/(2m+2)}$ . The condition that  $\sigma \leq 1$  is automatically satisfied. Ensuring that  $|\sigma| \leq 1$  is equivalent to the condition that the fraction on the right is less than two in magnitude. The special case for  $m = 1$  was given by (2.12). For  $m \geq 2$ , the extrema of the fraction occur at  $|k_x| = |k_y| = \theta^{-1/[2m+2]}$ , and implies that for unconditional stability we need  $\theta \geq \theta_m \equiv 2^{m-2}$ . Somewhat surprisingly, this result implies that for  $m > 2$  we must take  $\theta > 1$ , contrary to popular convention, which usually restricts  $\theta$  to  $0 \leq \theta \leq 1$  [38,49]. Consequently, for  $m > 2$  ( $hL_1$ ) yields an interesting counter-example to the conventional wisdom on  $\theta$ -weighted averages. For  $\theta < \theta_m$  Eq. (2.25) provides the condition for stability,  $\Delta t < \Delta x^{2m+2} (2^{m-1} - \theta - 2^{m/2} \sqrt{\theta_m - \theta}) / \theta^2$ . For an explicit method ( $\theta = 0$ ), this yields a very severe time-step restriction for large  $m$ ,  $\Delta t < 2(\Delta x / \sqrt{2})^{2m+2}$ .

### 2.4. Variable coefficient linear problems

As a next step towards solving nonlinear problems of the form (1.3), we briefly consider the case of fourth-order linear parabolic problems, with a prescribed coefficient function,  $f = f(x, y, t)$ , known for all values of position and time, namely

$$u_t + \nabla \cdot (f(x, y, t) \nabla \nabla^2 u) = 0. \tag{2.26}$$

This problem serves as a transition between the constant coefficient problem examined above and the fully nonlinear problems to be consider in the following sections. In fact, problems of the form (2.26) arise from linear stability analysis of solutions of the nonlinear problem (1.3). Moreover, (2.26) includes the full structure of the spatial operator needed for the nonlinear problems. As will be described later, careful consideration must be given to the spatial discretization of the diffusion coefficient in nonlinear degenerate problems [9]. Since much of the analysis follows from the discussion given above we present a concise summary of the results where attention will be focused on the new elements in the derivation of the ADI scheme. We restrict ourselves to the first-order fully implicit backward Euler scheme,

$$(\mathbf{I} + \Delta t \nabla \cdot [f^{n+1} \nabla \nabla^2]) u^{n+1} = u^n, \tag{2.27}$$

with the diffusion coefficient  $f^{n+1} = f(x, y, t^{n+1})$ . Using the same approximations as made in (2.1), we arrive at the approximate factorization of (2.27),

$$\mathbf{L}_x \mathbf{L}_y u^{n+1} = (\mathbf{I} - \Delta t (\partial_x [f^{n+1} \partial_{xyy}] + \partial_y [f^{n+1} \partial_{yxx}]) + \Delta t^2 \mathbf{D}_x \mathbf{D}_y) u^n, \quad (2.28)$$

where the one-dimensional operators  $\mathbf{L}_x, \mathbf{L}_y$  are given by (2.5) with  $\theta = 1$  and the differential operators are now defined as

$$\mathbf{D}_x = \partial_x [f^{n+1} \partial_{xxx}], \quad \mathbf{D}_y = \partial_y [f^{n+1} \partial_{yyy}]. \quad (2.29)$$

Note that the presence of the variable coefficient  $f(x, y, t)$  in (2.26) makes the one-dimensional spatial operators  $\mathbf{L}_x, \mathbf{L}_y$ , time-dependent and non-commutative. The variable coefficient also introduces a distinction between the two fourth-order mixed derivative terms, which were previously combined in (2.4). The ADI scheme for the variable coefficient problem takes the same general form as  $L_1$ ,

$$\begin{aligned} \mathbf{L}_x w &= -\Delta t \nabla \cdot (f^{n+1} \nabla \nabla^2 u^n), \\ (vL_1) \quad \mathbf{L}_y v &= w, \\ u^{n+1} &= u^n + v. \end{aligned} \quad (2.30)$$

### 3. Nonlinear equations

The remainder of this article focuses on ADI methods for the nonlinear problem

$$u_t + \nabla \cdot (f(u) \nabla \nabla^2 u) = 0, \quad (3.1)$$

in two dimensions. All of the ADI schemes for the linear problems in the previous sections fall under the heading of *non-iterative factorized methods* [64]. That is, the calculation of the approximate solution at the next time-step,  $u^{n+1}$ , required only a single application of the ADI scheme ( $(L_1)$ ,  $(vL_1)$  or  $(L_2)$ ) given the solution at the previous time-step,  $u^n$  (and  $u^{n-1}$  for  $(L_2)$ ). The accurate numerical solution of nonlinear problems, even in one dimension, generally necessitates the use of iterative schemes like Newton's method to converge to  $u^{n+1}$ . In general, solving multi-dimensional nonlinear problems like (3.1) using a backward Euler scheme [52], actually involves a combination of iterative processes [58];

- (i) (The “outer process”) Newton's method to converge to the solution of the discretized *nonlinear problem*.
- (ii) (The “inner process”) At each step of Newton's method, GMRES [39] or some other iterative method must be used to solve the *large sparse linear algebra problem* produced by the two-dimensional linearized operator (the Jacobian matrix).

Our use of approximate factorization-ADI schemes for the “inner process” reduces (ii) to a direct solution of the approximately factored problem. The “outer process” (i) must still be iterated to guarantee convergence to the solution. The resulting overall process can be described as an *iterative factorized method* [26,64]. In the following section we derive two classes of these methods for solving (3.1) and present them in a form that generalizes the structure of the previous schemes,  $(L_1)$ ,  $(vL_1)$ , and  $(L_2)$ . We will go on to compare these methods on a model nonlinear problem for two-dimensional thin film flow in Section 6.

### 3.1. Pseudo-linear factorization

Proceeding in a manner analogous to Sections 2 and 3, we derive a pseudo-linear factorization of the backward Euler method for (3.1),

$$\tilde{L}_x \tilde{L}_y u^{n+1} = u^n - (\Delta t (\partial_x [f(\tilde{u}^{n+1}) \partial_{xyy}] + \partial_y [f(\tilde{u}^{n+1}) \partial_{yxx}]) - \Delta t^2 \tilde{D}_x \tilde{D}_y) \tilde{u}^{n+1}, \tag{3.2}$$

where the linear operators are defined by

$$\tilde{L}_x = I + \theta \Delta t \tilde{D}_x, \quad \tilde{L}_y = I + \theta \Delta t \tilde{D}_y, \tag{3.3}$$

with  $\theta = 1$  for the backward Euler method, and the differential operators are given by

$$\tilde{D}_x \equiv \partial_x [f(\tilde{u}^{n+1}) \partial_{xxx}], \quad \tilde{D}_y \equiv \partial_y [f(\tilde{u}^{n+1}) \partial_{yyy}]. \tag{3.4}$$

Here the tildes refer to evaluation of the nonlinear coefficient function  $f(u)$  at some explicit approximation to the solution at  $t^{n+1}$ , call it  $\tilde{u}^{n+1}$ .  $\tilde{u}^{n+1}$  serves as a generalization of the linear estimate  $\bar{u}^{n+1}$  introduced in (2.16). We will describe more details about the choice of  $\tilde{u}^{n+1}$  shortly, but once it is given, (3.2) is a linear equation for  $u^{n+1}$ .

Proceeding formally, if we let  $v = u^{n+1} - \tilde{u}^{n+1}$  and subtract  $\tilde{L}_x \tilde{L}_y \tilde{u}^{n+1}$  from both sides of (3.2), we obtain

$$\tilde{L}_x \tilde{L}_y v = -(\tilde{u}^{n+1} - u^n) - \Delta t \nabla \cdot (f(\tilde{u}^{n+1}) \nabla \nabla^2 \tilde{u}^{n+1}). \tag{3.5}$$

The ADI split equations for this backward Euler method are then

$$\begin{aligned} \tilde{L}_x w &= -(\tilde{u}^{n+1} - u^n) - \Delta t \nabla \cdot (f(\tilde{u}^{n+1}) \nabla \nabla^2 \tilde{u}^{n+1}), \\ (pL_1) \quad \tilde{L}_y v &= w, \\ u^{n+1} &\sim \tilde{u}^{n+1} + v. \end{aligned} \tag{3.6}$$

If the exact solution  $u^{n+1}$  were known a priori, then it would serve as the correct value for  $\tilde{u}^{n+1}$ . Since this is not the case, we will think of  $(pL_1)$  as a linear iterative method with an initial estimate for  $u^{n+1}$  given by the trivial explicit first-order approximation  $\tilde{u}_{(0)}^{n+1} = u^n$ . Solving  $(pL_1)$  with this  $\tilde{u}^{n+1}$  yields an approximation of the solution at the next time-step that we will use as an improved estimate  $\tilde{u}_{(1)}^{n+1}$  in another iteration of  $(pL_1)$ ,

$$\tilde{u}_{(k+1)}^{n+1} = u_{(k)}^{n+1}, \quad k = 0, 1, 2, \dots \tag{3.7}$$

Similarly, we can derive a second-order pseudo-linear scheme using the BDF formula for the time derivative (2.13), and  $\theta = \frac{2}{3}$  in (3.3),

$$\begin{aligned} \tilde{L}_x w &= -\frac{1}{3}(3\tilde{u}^{n+1} - 4u^n + u^{n-1}) - \frac{2}{3} \Delta t \nabla \cdot (f(\tilde{u}^{n+1}) \nabla \nabla^2 \tilde{u}^{n+1}), \\ (pL_2) \quad \tilde{L}_y v &= w, \\ u^{n+1} &\sim \tilde{u}^{n+1} + v. \end{aligned} \tag{3.8}$$

For this method, our initial estimate can now be given by the second-order explicit two-level extrapolation,  $\tilde{u}_{(0)}^{n+1} = 2u^n - u^{n-1}$ .

If we do not iterate these methods at each time-step, then they are equivalent to  $(L_1)$ ,  $(L_2)$  with the time-lagged or extrapolated explicit coefficients for  $f(u)$ , hence we call them pseudo-linear approximations for (3.1). A similar ADI scheme was used by Dendy for the solution of a second-order nonlinear parabolic problem [19]. There, Dendy proved the convergence of the ADI scheme for a general class of second-order nonlinear parabolic problems without mixed derivatives.

### 3.2. Approximate-Newton method schemes

We pause from our examination of the use of ADI schemes for the inner process in the solution of (3.1) to examine the use of Newton’s method for the outer process. Consider solving (3.1) directly, using a backward Euler method. At each time-step, the discretized problem requires the solution of the system of nonlinear equations given by

$$F_1(u^{n+1}) \equiv u^{n+1} - u^n + \Delta t \nabla \cdot (f(u^{n+1}) \nabla \nabla^2 u^{n+1}) = 0. \tag{3.9}$$

Applying Newton’s method to solve this nonlinear system yields the iterative method,

$$\mathbf{J}(\tilde{u}_{(k)}^{n+1})v = -F_1(\tilde{u}_{(k)}^{n+1}), \quad v = \tilde{u}_{(k+1)}^{n+1} - \tilde{u}_{(k)}^{n+1}, \tag{3.10}$$

for  $k = 0, 1, 2, \dots$ , where the Jacobian, or functional derivative, of the nonlinear system is the linearized operator,

$$\mathbf{J}(u^{n+1})v \equiv \frac{\delta F_1}{\delta u} v = v + \Delta t \nabla \cdot (v f'(u^{n+1}) \nabla \nabla^2 u^{n+1} + f(u^{n+1}) \nabla \nabla^2 v). \tag{3.11}$$

For  $\tilde{u}^{n+1}$  sufficiently close to  $u^{n+1}$ , the sequence  $\{\tilde{u}_{(k)}^{n+1}\}$  converges quadratically to the exact solution  $u^{n+1}$ . This approach was employed by Oron [52] to solve a thin film problem in two dimensions, where a GMRES iterative method was used to solve the linear problem connected with the large sparse Jacobian matrix  $\mathbf{J}$ . As described in [52], this approach for the inner iterative process can be computationally expensive and may become the limiting factor in the speed and resolution of numerical simulations for these problems.

To develop a more computationally efficient approach, we consider an approximate Newton method, where the Jacobian is approximated by a factorized operator,  $\mathbf{J} \sim \mathbf{A} \equiv \tilde{\mathbf{L}}_x \tilde{\mathbf{L}}_y$ , with the “one-dimensional” linearized operators given by (3.3) with  $\theta = 1$ , and the differential operators given by

$$\begin{aligned} \tilde{\mathbf{D}}_x \phi &= \partial_x [\phi f'(\tilde{u}^{n+1}) \partial_x \nabla^2 \tilde{u}^{n+1} + f(\tilde{u}^{n+1}) \partial_{xxx} \phi], \\ \tilde{\mathbf{D}}_y \phi &= \partial_y [\phi f'(\tilde{u}^{n+1}) \partial_y \nabla^2 \tilde{u}^{n+1} + f(\tilde{u}^{n+1}) \partial_{yyy} \phi]. \end{aligned} \tag{3.12}$$

Then we have the first-order ADI–Newton method

$$\begin{aligned} \tilde{\mathbf{L}}_x w &= -F_1(\tilde{u}^{n+1}), \\ (N_1) \quad \tilde{\mathbf{L}}_y v &= w, \\ \tilde{u}_{(k+1)}^{n+1} &= \tilde{u}_{(k)}^{n+1} + v. \end{aligned} \tag{3.13}$$

Note that apart from the differences in the definitions of the differential operators,  $\tilde{\mathbf{D}}_x, \tilde{\mathbf{D}}_y$ , given by (3.4) and (3.12), the two schemes  $(pL_1)$  and  $(N_1)$  are equivalent in structure. We note that the operators (3.12) for  $(N_1)$  in fact contain explicitly evaluated mixed derivative terms present only for problems with non-constant coefficient functions  $f(u)$ . It is hoped that keeping these terms yields a better approximation of the Jacobian and improves convergence of the scheme  $(N_1)$  relative to  $(pL_1)$ . In particular, it is noteworthy that if the solution of (3.1) is independent of one direction in space, that is  $u = u(x, t)$  or  $u = u(y, t)$ , then  $(N_1)$  becomes identical with Newton’s method. In this case,  $(N_1)$  would converge quadratically, while  $(pL_1)$  converges linearly. We also note that the construction for  $(N_1)$  can be applied to strongly nonlinear problems like (1.1), while  $(pL_1)$  is limited to quasilinear problems like (3.1).

The scheme  $(N_1)$  generalizes to yield other ADI–Newton methods simply by replacing  $F(u)$  and  $\theta$  appropriately:

- (i) The second-order BDF scheme ( $N_2$ ) comparable to ( $pL_2$ ) results from the choice  $\theta = 2/3$  in (3.3) and

$$F_2(u^{n+1}) \equiv u^{n+1} - \frac{1}{3}(4u^n - u^{n-1}) + \frac{2}{3}\Delta t \nabla \cdot (f(u^{n+1})\nabla \nabla^2 u^{n+1}). \tag{3.14}$$

- (ii) There are two variants of the second-order Crank–Nicolson scheme with  $\theta = 1/2$  for the nonlinear problem. One, called a trapezoidal scheme, ( $N_T$ ) is given by an average of the spatial operator at explicit and implicit time-steps,

$$F_T(u^{n+1}) \equiv u^{n+1} - u^n + \frac{1}{2}\Delta t [\nabla \cdot (f(u^{n+1})\nabla \nabla^2 u^{n+1}) + \nabla \cdot (f(u^n)\nabla \nabla^2 u^n)]. \tag{3.15}$$

The other, called a midpoint scheme, ( $N_M$ ) is given by the spatial operator applied to the average of the time-steps,

$$F_M(u^{n+1}) \equiv u^{n+1} - u^n + \Delta t \left[ \nabla \cdot \left( f \left( \frac{1}{2}[u^{n+1} + u^n] \right) \nabla \nabla^2 \frac{1}{2}[u^{n+1} + u^n] \right) \right]. \tag{3.16}$$

The formal second-order accuracy of the ( $N_T$ ) and ( $N_M$ ) schemes does not contradict Beam and Warming’s result that one-step second-order accurate methods are not possible with mixed derivatives [5]. Their result applies only to *non-iterative* ADI methods. Consequently, the first iterate  $\tilde{u}_{(1)}^{n+1}$  can at best be a first-order accurate solution, but with further iteration,  $\tilde{u}_{(k)}^{n+1}$  converges to a second-order accurate solution at each time-step.

In general these ADI methods are all fundamentally linear iterative methods to solve  $F(u^{n+1}) = 0$  with an approximate factorization used for the iteration operator matrix. We now briefly discuss issues related to the convergence of these iterative methods. Rather than providing proofs specific to our schemes, we will cast the schemes in the framework for general iterative methods for solving systems of nonlinear equations and reference applicable results from that body of literature [39,58].

For convenience of the following discussion, we simplify our notation for the iterates from  $\tilde{u}_{(k)}^{n+1}$  to just  $u_k$  and refer to the exact solution of  $F(u^{n+1}) = 0$  as the fixed point  $u_*$ . Then we can write the ADI–Newton schemes in the form

$$u_{k+1} = u_k - A_k^{-1}F(u_k), \quad A_k \equiv A(u_k) = \tilde{L}_x \tilde{L}_y. \tag{3.17}$$

This takes the form of a general single-step iterative method,  $u_{k+1} = G(u_k)$ . Convergence to the fixed point  $u_*$  will occur if  $\|\delta_u G(u_*)\| < 1$ , where

$$\frac{\delta G}{\delta u} = I - \delta_u(A^{-1}F). \tag{3.18}$$

For Newton’s method,  $A = J$  yielding  $\|\delta_u G(u_*)\| = 0$ , and we get quadratic convergence. In general, this convergence rate won’t apply for the approximation factorizations used in our ADI schemes, but we can hope to show that the schemes are convergent under reasonable assumptions. Indeed, (3.17) will converge if

$$\|\delta_u G(u_k)\| = \|I - A_k^{-1}J_k\| < 1, \tag{3.19}$$

as shown by Dennis [20] for Newton-like methods, and considered in connection with a class of inexact Newton methods in [18]. Using the Schwartz inequality, this condition can be established if

$$\|A_k^{-1}\| \cdot \|E_k\| \leq 1, \tag{3.20}$$

where  $E$  is the error in the iteration operator [39,40]. For the ADI–Newton schemes, this is given by

$$E \equiv J - A = \theta \Delta t (\partial_x [f(u) \partial_{xyy}] + \partial_y [f(u) \partial_{yxx}]) + O(\Delta t^2), \tag{3.21}$$

where  $A = I + O(\Delta t)$ . For the linear constant coefficient problem, with  $f(u) = 1$ , (3.20) can be established in a straightforward manner using Fourier analysis to recover the linear stability results found earlier. For the nonlinear problem, given sufficient smoothness of  $u$ , similar bounds could be expected to apply, but there may be additional restrictions on  $\Delta t$  to ensure convergence. A similar analysis of Newton-like methods for time-dependent nonlinear convection–diffusion equations was briefly given in [32]. We leave the details of the analysis of the convergence of these schemes for further study.

#### 4. Spatial discretization and boundary conditions

To complete the formulation of the ADI schemes, we present the details of a second-order finite difference spatial discretization and briefly discuss boundary conditions. For smooth solutions of the diffusion equations we consider, consistent spatial discretizations should not significantly alter the results obtained using the continuous spatial operators. Hence to streamline our presentation, we have neglected these considerations until now. Without loss of generality, the influence of spatial discreteness can be incorporated back into the stability results, (2.12) and (2.20) by appropriately re-defining the wave-vector  $k$  in terms of finite difference derivative operators, [2,34].

While ADI methods can be applied directly on any Cartesian cross product mesh,  $\{u(\mathbf{x}_{i,j}, t^n) = u_{i,j}^n \mid \mathbf{x}_{i,j} = (x_i, y_j)\}$ , for clarity of presentation, we will use a uniform rectangular mesh with  $x_i = i \Delta x$ ,  $y_j = j \Delta y$ . For the linear constant-coefficient problem (2.1), we can discretize the spatial operators in terms of

$$\delta_{xx} u_{i,j} \equiv \frac{u_{i+1,j} - 2u_{i,j} + u_{i-1,j}}{\Delta x^2} = \partial_{xx} u(x_i, y_j) + O(\Delta x^2), \tag{4.1}$$

$$\delta_{xxxx} u_{i,j} \equiv \frac{u_{i+2,j} - 4u_{i+1,j} + 6u_{i,j} - 4u_{i-1,j} + u_{i-2,j}}{\Delta x^4} = \partial_{xxxx} u(x_i, y_j) + O(\Delta x^2), \tag{4.2}$$

and similarly for  $\delta_{yy}$  and  $\delta_{yyyy}$ . Consequently, the standard thirteen-point stencil for the biharmonic operator [1,38] is therefore

$$\nabla^4 u(x_i, y_j) = \delta_{xxxx} u_{i,j} + 2\delta_{xx} \delta_{yy} u_{i,j} + \delta_{xxxx} u_{i,j} + O(\Delta x^2) + O(\Delta y^2), \tag{4.3}$$

and the spatial discretizations of the one-dimensional operators (2.5) are given by

$$L_x = (I + \theta \Delta t \delta_{xxxx}) + O(\Delta t \Delta x^2), \quad L_y = (I + \theta \Delta t \delta_{yyyy}) + O(\Delta t \Delta y^2). \tag{4.4}$$

Using this discretization, the ADI schemes ( $L_1$ ) and ( $L_2$ ) involve only the solution of sets of pentadiagonal banded matrices.

Solution of the variable-coefficient linear problem (2.26) and the nonlinear problem (3.1) are only slightly more complicated as they involve computation of first derivatives of a third order flux,  $\mathbf{Q} = (p, q)^T \equiv f \nabla \nabla^2 u$ . To maintain a finite difference stencil analogous to the biharmonic operator, we use the second-order centered difference for the first derivatives of the flux,  $\delta_x p_{i,j} \equiv (p_{i+1/2,j} - p_{i-1/2,j}) / \Delta x = \partial_x p(x_i, y_j) + O(\Delta x^2)$ , and similarly for  $\delta_y q_{i,j}$ . We note that a similar discretization for the strongly nonlinear equation (1.1) would require a stencil of twenty-one rather than thirteen points since  $H$  (1.2) includes mixed derivatives terms not present in  $\nabla^2 u$ .

The discretization of the flux also depends on the approximations used for the diffusion coefficient. Ideally, the exact cell-centered values of  $f$  at time  $t^{n+1}$ ,  $f_{i+1/2,j}^{n+1} = f(u(x_{i+1/2}, y_j, t^{n+1}))$  can be used in (2.27) and in the flux. However, depending on the constraints of available information, other approximations may be made. If only values of  $f$  on grid points can be used, a trapezoidal average can be employed [21],

$$f_{i+1/2,j} = \frac{1}{2}[f(u_{i,j}) + f(u_{i+1,j})] + O(\Delta x^2). \quad (4.5)$$

For nonlinear problems with  $f = f(u)$ , trapezoidal averages, and midpoint rules of the form

$$f_{i+1/2,j} = f\left(\frac{1}{2}[u_{i,j} + u_{i+1,j}]\right) + O(\Delta x^2), \quad (4.6)$$

have been commonly used. However, recent studies have shown that a different approximation, one resembling an inverse derivative of a potential function,

$$f_{i+1/2,j} = \frac{u_{i+1,j} - u_{i,j}}{F(u_{i+1,j}) - F(u_{i,j})} \quad \text{where } F(u) = \int \frac{du}{f(u)}, \quad (4.7)$$

more faithfully reproduce some aspects of the behavior of the PDE. In [67], *entropy dissipating schemes* based on this approximation were shown to properly dissipate energy and preserve positivity of solutions [9,21,33].

While relevant boundary conditions for (2.1) and (3.1) vary somewhat depending on intended applications, for problems in fluid and solid mechanics, several sets of boundary conditions commonly occur. For these fourth-order problems, Dirichlet conditions specify the value of  $u$  and the second normal derivative  $\partial_{nn}u$  on the boundary of the domain. For the motion of plates described by (2.1), homogeneous Dirichlet conditions describe simply-supported edges. For (3.1), inhomogeneous Dirichlet conditions in one dimension were called pressure boundary conditions [13,25]. This is an appropriate terminology since specifying a constant film thickness at the boundary,  $u = c_1$ , simplifies the form of the pressure at the boundary,  $P \equiv \nabla^2 u = \partial_{nn}u = c_2$ . Mass preserving no-flux boundary conditions are specified by  $\mathbf{n} \cdot \mathbf{Q} = 0$ , where  $\mathbf{n}$  is the unit outward normal. This condition is used to describe fluid layers confined in a finite container, and also for free edges of vibrating plates. For thin film problems, a contact angle condition must also be specified at a boundary; the contact angle can be specified by the normal derivative of the film thickness at the boundary,  $\partial_n u = \cot \phi$ . Specifying a fixed contact angle,  $\partial_n u = c_3$ , reduces the normal component of the flux,  $f(u)\partial_n \nabla^2 u$ , to  $f(u)\partial_{nnn}u$ . These Neumann boundary conditions were used in [66] with  $\partial_n u = 0$  to neglect any meniscus at the boundary. Since both of these Neumann and Dirichlet boundary conditions are separable in terms of normal and tangent directions, they are straightforward to implement in the ADI schemes using standard approaches from one-dimensional problems. Periodic boundary conditions, as used in [60], yield sparse cyclic matrices but these problems can be solved with ADI schemes using penta-diagonal matrices via the Sherman–Morrison formula [57]. We note that some information on using ADI methods with curved boundaries and non-rectangular domains is given in [47,49].

## 5. Numerical experiments

We conclude by presenting simulations of nonlinear problems for the dynamics of thin films calculated using the ADI schemes constructed above. We begin with a fundamental test problem [3,21,33] used to

verify the order of accuracy of the ADI schemes and to demonstrate convergence of the solution to the dynamic scaling law for the known self-similar solution. The second example illustrates interesting pattern formation and spatial structure developed in a problem with dynamics controlled by a balance between the fourth-order operator in (3.1) and lower order terms representing other physical effects. We note that our ADI schemes are also being used for other studies on undercompressive shocks in thin films [12].

### 5.1. A nonlinear test problem: Convergence to a self-similar solution

The thin film equation (3.1) with  $f(u) = u$ ,

$$u_t + \nabla \cdot (u \nabla \nabla^2 u) = 0, \quad (5.1)$$

has a well-known closed-form compactly-supported,  $d$ -dimensional radially-symmetric self-similar solution [31] given by

$$u(r, t) = \frac{1}{8(d+2)\tau^d} (L^2 - \eta^2)_+^2, \quad 0 \leq \eta \leq L, \quad (5.2)$$

with  $u \equiv 0$  for  $\eta > L$ , and

$$\tau = [(d+4)(t+t_0)]^{1/(d+4)}, \quad \eta = r/\tau, \quad (5.3)$$

where  $r = x$  in one dimension ( $d = 1$ ) and  $r = \sqrt{x^2 + y^2}$  for  $d = 2$ . This solution, found by Smyth and Hill [61] for  $d = 1$ , is the higher-order analogue of the Barenblatt–Pattle similarity solution for the porous medium equation. However, unlike the porous medium equation, the numerical simulation of higher-order nonlinear degenerate diffusion equations like (5.1) require careful analysis [7,9] and highly specialized numerical schemes in order to preserve non-negativity [3,33] or positivity [9,21,67] of the solution. Simulation of the similarity solution for the one-dimensional version of (5.1) using a non-negativity preserving scheme was carried out in [33]. We will not pursue the discussion of these specialized numerical schemes here other than to say that the method given by [67] could be easily incorporated into our ADI schemes. Instead, we will use the analytic regularization of (5.1) shown by [7] to preserve positivity. We replace the coefficient function  $f(u) = u$  by

$$f_\varepsilon(u) = \frac{u^5}{\varepsilon u + u^4}, \quad (5.4)$$

so that  $f_\varepsilon(u) \sim u$  for  $u \gg \varepsilon$  and begin with positive initial data; the solution of this problem should remain positive for all times. We take the initial data,

$$u_0(x, y) = \delta + e^{-\sigma(x^2+y^2)}, \quad (5.5)$$

where  $\delta > 0$  represents the thickness of an ultra-thin precursor layer under the Gaussian fluid droplet centered at the origin.

We solve (5.1) using a  $100 \times 100$  discrete grid on the unit square and Neumann boundary conditions on all edges, with the parameters  $\varepsilon = 10^{-9}$ ,  $\delta = 10^{-2}$ , and  $\sigma = 80$ . In Fig. 1 we show convergence of the solution in the limit that the time-step vanishes,  $\Delta t \rightarrow 0$ . We verified the orders of accuracy expected for the ADI schemes for this problem. In this plot, a simple measure of the error in the solution was used—the difference between the height of the droplet at time  $T = 10^{-4}$ ,  $u(0, T)$ , compared with a very

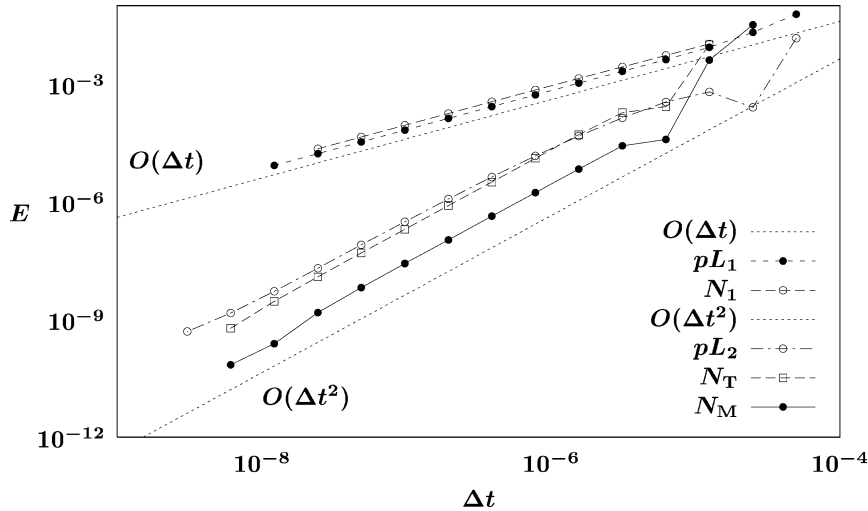


Fig. 1. Convergence of the ADI schemes to a solution of the problem (5.1) at a finite time  $T$  as  $\Delta t \rightarrow 0$ . First-order schemes: pseudo-linear ( $pL_1$ ) (3.6), Newton ( $N_1$ ) (3.13); Second-order schemes: pseudo-linear ( $pL_2$ ) (3.8), Newton-trapezoidal ( $N_T$ ) (3.15), and Newton-midpoint ( $N_M$ ) (3.16).

accurate extrapolated value obtained from a ( $N_T$ ) simulation,  $\bar{u}(0, T)$ , i.e.,  $E = |u(0, T) - \bar{u}(0, T)|$ . As shown in Fig. 1, the respective first and second-order accurate methods showed the rate of convergence expected up to a maximum time-step of approximately  $\Delta t \approx 10^{-5}$ . While the ADI schemes were shown to be unconditionally stable for the linear constant coefficient problem, we should not expect this to hold for nonlinear problems, where stability and convergence become solution-dependent issues. We note that while  $\Delta t \approx 10^{-5}$  may seem to be a small time-step, in comparison, an explicit forward Euler method for this problem did not converge for any time-step bigger than  $\Delta t \approx 2 \times 10^{-13}$ . Note that this constraint on the time-step is much tighter than the upper bound  $\Delta t = O(\Delta x^4) = O(10^{-8})$  expected from linear analysis; this illustrates the strong nonlinearity of (5.1).

With regard to the first-order methods, surprisingly the (non-iterative) pseudo-linear scheme (3.6) outperforms the first-order approximate Newton method (3.13). Furthermore, it was found that iterating the ( $pL_1$ ) scheme did not provide measurable improvement. In contrast, for the second-order accurate methods, the pseudo-linear scheme ( $pL_2$ ) was not as accurate as the approximate Newton methods. Again, no measurable improvement was noted in the results from the multistep pseudo-linear scheme by using it iteratively. At a given size time-step, the pseudo-linear scheme had comparable but slightly large errors than the Newton-trapezoid scheme (3.15). In comparison, the errors for the Newton-midpoint scheme (3.16) are an order of magnitude smaller. Since it does not require the storage of the solution at additional time-steps, the ( $N_M$ ) scheme uses less memory than ( $pL_2$ ). If fewer than four iterations per time-step are needed, the Newton scheme is also more computationally efficient than ( $pL_2$ ) for a given error tolerance. A similar comparison with ( $pL_1$ ) suggests that at the same level of accuracy, a Newton-midpoint code could be roughly one thousand times faster. For problems where a somewhat larger error is acceptable the non-iterative pseudo-linear scheme ( $pL_2$ ) may be the most efficient numerical method.

In this problem, the maximum of the solution remains at the origin for all times and Fig. 2(a) shows how the droplet height evolves as a function of time. In carrying out simulations for longer times shown in Fig. 2, we took advantage of adaptive time-stepping by adjusting  $\Delta t$  in connection with maintaining

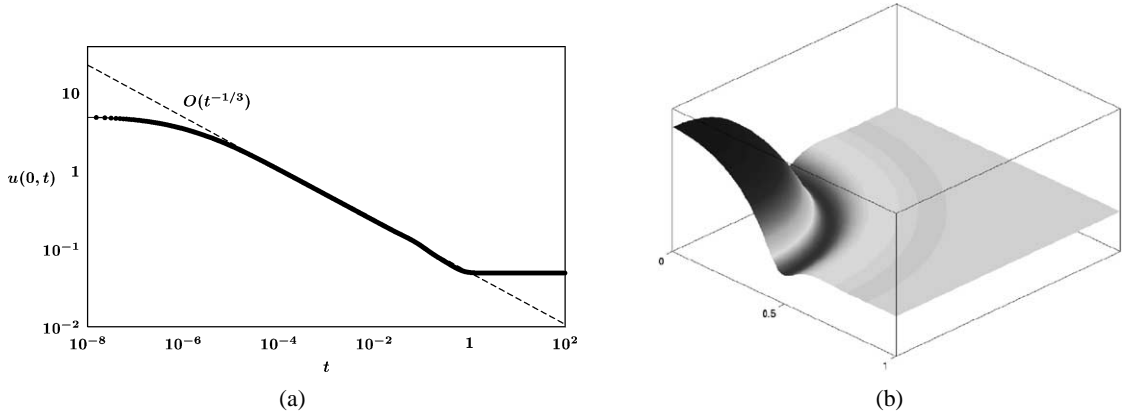


Fig. 2. (a) The time evolution of the droplet height in the nonlinear test problem on the unit square. (b) The numerical approximately-radially-symmetry self-similar solution of the regularized problem shown in a linear<sup>2</sup>-log graph to resolve the fine-scale oscillatory structure of the thin film.

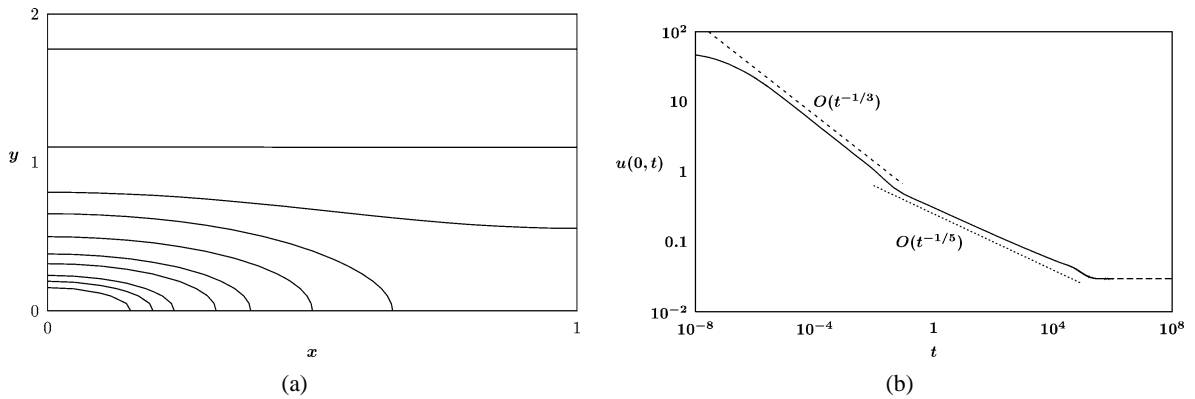


Fig. 3. (a) Mid-height contours of the initially circular spreading droplet in a large rectangular domain,  $0 \leq x \leq 1$ ,  $0 \leq y \leq 20$ . (b) Evolution of the droplet height showing the intermediate asymptotics for the  $d = 2$  and  $d = 1$  self-similar solutions.

a uniform convergence criterion for terminating the Newton iterations at each time-step [39], requiring that  $\|F(u_{(K)}^{n+1})\|$  be less than some fixed tolerance for a fixed number of iterations  $K$ .

After an initial transient, for  $t > 10^{-5}$  the solution of (5.1), (5.5) converges to a regularized form of the similarity solution (5.2) as in borne out by the height of the drop following  $u(0, t) = O(t^{-1/3})$ . The spatial structure of the solution is shown in Fig. 2(b). For  $u \gg \delta$ , the solution approaches (5.2); for  $u \sim \delta$ , there is an oscillatory connection to the surrounding ultra-thin film layer. The oscillations are a real feature of the solution, caused by the regularizations  $(\epsilon, \delta)$ , and have been studied using asymptotic analysis by King and Bowen [43]. For large times,  $t > 10^{-1}$ , the evolution is dominated by the boundary conditions and the solution is no longer radially symmetric as it approaches a uniform flat state. This behavior is also illustrated in Fig. 3, which shows results for a simulation with the same initial conditions on a domain with a large aspect ratio,  $0 \leq x \leq 1$  and  $0 \leq y \leq 20$ . For short times, the solution evolves like the  $d = 2$  radially symmetric similarity solution. For longer times, gradients across the narrow dimension of the

domain approach zero, and the solution approaches a one-dimensional form,  $u = u(y, t)$  and evolves like the  $d = 1$  similarity solution with  $u(0, t) = O(t^{-1/5})$ .

### 5.2. Pattern formation in dewetting films

Very thin films coating solid surfaces are unstable to perturbations that produce non-uniformities, see [10,54,60,66] and references therein. A lubrication theory model for this physical behavior is given by a thin film equation with  $f(u) = u^3$  and an additional disjoining pressure [10,54],

$$u_t + \nabla \cdot (u^3 \nabla [\nabla^2 u - \mathcal{P}(u)]) = 0. \quad (5.6)$$

A simple model for the intermolecular forces between the solid substrate and the fluid film can be described by a disjoining pressure of the form

$$\mathcal{P}(u) = \frac{1}{u^3} \left( 1 - \frac{\varepsilon}{u} \right). \quad (5.7)$$

In [10] it was shown that other models for the pressure, including the standard Lennard–Jones potential [55], yield qualitatively similar behavior. The parameter  $\varepsilon$  in (5.7) sets a scale for the minimum film thickness. If  $\varepsilon = 0$  then finite-time rupture occurs, with a singularity developing when  $u \rightarrow 0$  at a point (see Fig. 4(a) along with [66] and references therein). In [66], rupture of two-dimensional thin films was simulated using the ADI schemes developed here. In particular, some of the figures in [66] were calculated using the  $(N_1)$  ADI scheme on grids with  $500 \times 500$  up to  $2000 \times 2000$  points on the unit square.

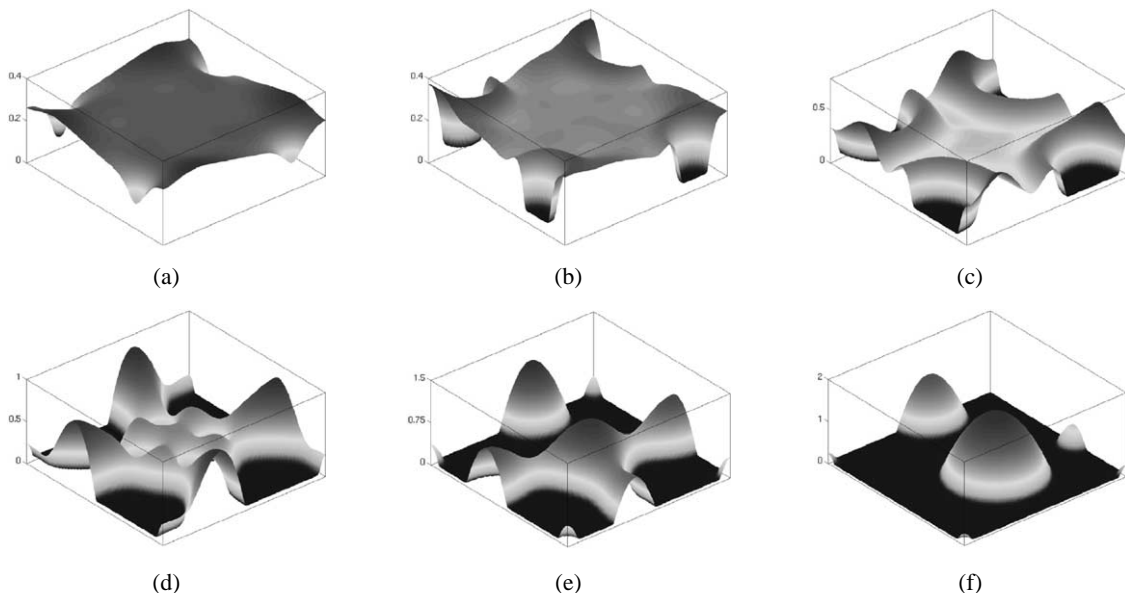


Fig. 4. Stages in the dewetting of a two-dimensional thin film; (a) formation of rupture points, (b) nucleation of dry-spots or “holes”, (c) further dewetting producing a ridge network, (d) break-up of some ridges, (e) co-existence of fluid droplets and ridges, (f) final stages of coarsening with only droplets.

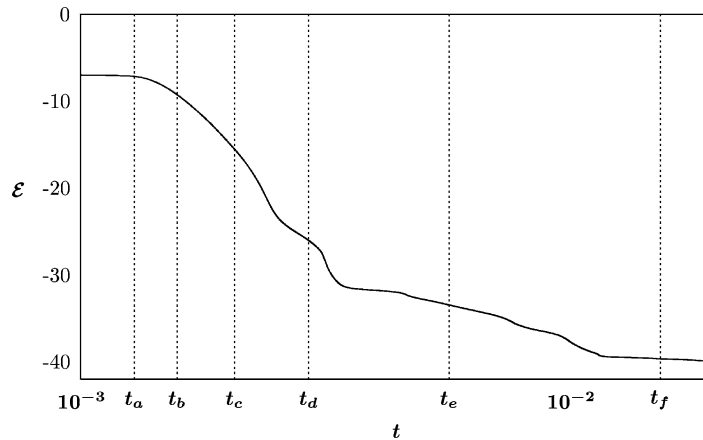


Fig. 5. Monotone decreasing energy of the solution of the dewetting model (5.6). Times corresponding to the stages of evolution in Fig. 4 are indicated.

For  $\varepsilon > 0$ , complete rupture does not occur, but the process of forming regions where the film thickness decreases to  $O(\varepsilon)$  is called dewetting. Dewetting leads to the formation of evolving spatial patterns with competition between droplets and fluid ridges [10,60] (see Fig. 4(d), (e)). Some stages from this evolution process are shown in Fig. 4. These results were calculated using the  $(N_T)$  ADI scheme for (5.7), (5.6) with  $\varepsilon = 0.05$  where Neumann boundary conditions are applied to a  $100 \times 100$  point mesh on the unit square. Note that the inclusion of the second-order terms due to  $P(u)$  from (5.6) introduce no difficulties in the ADI scheme. This problem has an energy functional,

$$\mathcal{E} = \iint \frac{1}{2} |\nabla u|^2 + Q(u) \, dy \, dx, \quad Q(u) = - \int_u^\infty P(v) \, dv. \quad (5.8)$$

The energy is monotone decreasing for all solutions of (5.6) [10]; in Fig. 5 we show that the ADI simulation correctly reproduces this property of the dynamics. A similar dewetting model including evaporative effects was studied by Schwartz et al. [60] to describe patterns in drying thin films, calculated using an ADI scheme on a periodic domain. For these problems, questions of interest focus on complex pattern formation, geometric instabilities, and the dynamics of topological transitions. Some aspects are tractable analytically, but progress on most fronts requires insight that must be gained from numerical simulation.

## Acknowledgement

We thank Andrea Bertozzi for suggesting this project and for many helpful conversations. This research was supported by NSF grant FRG-DMS 0074049 and ONR grant N-00140110290. TW was also supported by a fellowship from the Alfred P. Sloan Foundation.

## References

- [1] M. Abramowitz, I.A. Stegun (Eds.), *Handbook of Mathematical Functions with Formulas, Graphs, and Mathematical Tables*, Dover, New York, 1992.
- [2] J. Augenbaum, S.E. Cohn, D. Marchesin, Eliminating grid-orientation errors in alternating-direction implicit schemes, *Appl. Numer. Math.* 8 (1) (1991) 1–10.
- [3] J.W. Barrett, J.F. Blowey, H. Garcke, Finite element approximation of a fourth-order nonlinear degenerate parabolic equation, *Numer. Math.* 80 (4) (1998) 525–556.
- [4] R.M. Beam, R.F. Warming, An implicit finite-difference algorithm for hyperbolic systems in conservation-law form, *J. Comput. Phys.* 22 (1) (1976) 87–110.
- [5] R.M. Beam, R.F. Warming, Alternating direction implicit methods for parabolic equations with a mixed derivative, *SIAM J. Sci. Statist. Comput.* 1 (1) (1980) 131–159.
- [6] D.J. Benney, Long waves on liquid films, *J. Math. Phys.* 45 (1966) 150–155.
- [7] F. Bernis, A. Friedman, Higher order nonlinear degenerate parabolic equations, *J. Differential Equations* 83 (1) (1990) 179–206.
- [8] A.J. Bernoff, A.L. Bertozzi, T.P. Witelski, Axisymmetric surface diffusion: dynamics and stability of self-similar pinchoff, *J. Statist. Phys.* 93 (3–4) (1998) 725–776.
- [9] A.L. Bertozzi, The mathematics of moving contact lines in thin liquid films, *Notices Amer. Math. Soc.* 45 (6) (1998) 689–697.
- [10] A.L. Bertozzi, G. Grün, T.P. Witelski, Dewetting films: bifurcations and concentrations, *Nonlinearity* 14 (6) (2001) 1569–1592.
- [11] A.L. Bertozzi, M.C. Pugh, Long-wave instabilities and saturation in thin film equations, *Comm. Pure Appl. Math.* 51 (6) (1998) 625–661.
- [12] M. Bowen, A.L. Bertozzi, Transient behaviour of two-dimensional undercompressive shocks, Preprint, 2001.
- [13] P. Constantin, T.F. Dupont, R.E. Goldstein, L.P. Kadanoff, M.J. Shelley, S.-M. Zhou, Droplet breakup in a model of the Hele–Shaw cell, *Phys. Rev. E* (3) 47 (6) (1993) 4169–4181.
- [14] S.D. Conte, Numerical solution of vibration problems in two space variables, *Pacific J. Math.* 7 (1957) 1535–1544.
- [15] S.D. Conte, R.T. Dames, An alternating direction method for solving the biharmonic equation, *Math. Tables Aids Comput.* 12 (1958) 198–205.
- [16] S.D. Conte, R.T. Dames, On an alternating direction method for solving the plate problem with mixed boundary conditions, *J. Assoc. Comput. Mach.* 7 (1960) 264–273.
- [17] I.J.D. Craig, A.D. Sneyd, An alternating-direction implicit scheme for parabolic equations with mixed derivatives, *Comput. Math. Appl.* 16 (4) (1988) 341–350.
- [18] R.S. Dembo, S.C. Eisenstat, T. Steihaug, Inexact Newton methods, *SIAM J. Numer. Anal.* 19 (2) (1982) 400–408.
- [19] J.E. Dendy, Jr, Alternating direction methods for nonlinear time-dependent problems, *SIAM J. Numer. Anal.* 14 (2) (1977) 313–326.
- [20] J.E. Dennis, Jr, On Newton-like methods, *Numer. Math.* 11 (1968) 324–330.
- [21] J.A. Diez, L. Kondic, A.L. Bertozzi, Global models for moving contact lines, *Phys. Rev. E* 63 (1) (2001) 011208.
- [22] M.P. do Carmo, *Differential Geometry of Curves and Surfaces*, Prentice-Hall, Englewood Cliffs, NJ, 1976.
- [23] J. Douglas, Jr, J.E. Gunn, A general formulation of alternating direction methods. I. Parabolic and hyperbolic problems, *Numer. Math.* 6 (1964) 428–453.
- [24] J. Douglas, Jr, H.H. Rachford, Jr, On the numerical solution of heat conduction problems in two and three space variables, *Trans. Amer. Math. Soc.* 82 (1956) 421–439.
- [25] T.F. Dupont, R.E. Goldstein, L.P. Kadanoff, S.-M. Zhou, Finite-time singularity formation in Hele–Shaw systems, *Phys. Rev. E* (3) 47 (6) (1993) 4182–4196.
- [26] C. Eichler-Liebenow, P.J. van der Houwen, B.P. Sommeijer, Analysis of approximate factorization in iteration methods, *Appl. Numer. Math.* 28 (2–4) (1998) 245–258.
- [27] C.M. Elliott, D.A. French, Numerical studies of the Cahn–Hilliard equation for phase separation, *IMA J. Appl. Math.* 38 (2) (1987) 97–128.
- [28] M.H. Eres, L.W. Schwartz, R.V. Roy, Fingering phenomena for driven coating films, *Phys. Fluids* 12 (6) (2000) 1278–1295.

- [29] M.H. Eres, D.E. Weidner, L.W. Schwartz, Three-dimensional direct numerical simulation of surface tension gradient effects on the leveling of an evaporating multicomponent fluid, *Langmuir* 15 (1999) 1859–1871.
- [30] G. Fairweather, A.R. Gourlay, Some stable difference approximations to a fourth-order parabolic partial differential equation, *Math. Comp.* 21 (1967) 1–11.
- [31] R. Ferreira, F. Bernis, Source-type solutions to thin-film equations in higher dimensions, *European J. Appl. Math.* 8 (5) (1997) 507–524.
- [32] K. Georg, D. Zachmann, Nonlinear convection diffusion equations and Newton-like methods, in: K. Georg, E.A. Allgower (Eds.), *Computational Solution of Nonlinear Systems of Equations* (Fort Collins, CO, 1988), American Mathematical Society, Providence, RI, 1990, pp. 237–256.
- [33] G. Grün, M. Rumpf, Nonnegativity preserving convergent schemes for the thin film equation, *Numer. Math.* 87 (1) (2000) 113–152.
- [34] C. Hirsch, *Numerical Computation of Internal and External Flows*, Vol. I, Wiley, New York, 1988.
- [35] W.H. Hundsdorfer, A note on stability of the Douglas splitting method, *Math. Comp.* 67 (221) (1998) 183–190.
- [36] W.H. Hundsdorfer, J.G. Verwer, Stability and convergence of the Peaceman–Rachford ADI method for initial-boundary value problems, *Math. Comp.* 53 (187) (1989) 81–101.
- [37] J.M. Hyman, B. Nicolaenko, S. Zaleski, Order and complexity in the Kuramoto–Sivashinsky model of weakly turbulent interfaces, *Phys. D* 23 (1–2) (1986) 265–292.
- [38] A. Iserles, *A First Course in the Numerical Analysis of Differential Equations*, Cambridge University Press, Cambridge, 1996.
- [39] C.T. Kelley, *Iterative Methods for Linear and Nonlinear Equations*, SIAM, Philadelphia, PA, 1995.
- [40] C.T. Kelley, C.T. Miller, M.D. Tocci, Termination of Newton/chord iterations and the method of lines, *SIAM J. Sci. Comput.* 19 (1) (1998) 280–290.
- [41] J.R. King, Emerging areas of mathematical modelling, *Philos. Trans. Roy. Soc. London Ser. A Math. Phys. Engrg. Sci.* 358 (1765) (2000) 3–19.
- [42] J.R. King, Two generalisations of the thin film equation, *Math. Comput. Modelling* 34 (7–8) (2001) 737–756.
- [43] J.R. King, M. Bowen, Moving boundary problems and non-uniqueness for the thin film equation, *European J. Appl. Math.* 12 (3) (2001) 321–356.
- [44] G.I. Marchuk, Splitting and alternating direction methods, in: P.G. Ciarlet, J.-L. Lions (Eds.), *Handbook of Numerical Analysis Vol. I*, North-Holland, Amsterdam, 1990, pp. 197–462.
- [45] S. McKee, A.R. Mitchell, Alternating direction methods for parabolic equations in two space dimensions with a mixed derivative, *Comput. J.* 13 (1970) 81–86.
- [46] S. McKee, D.P. Wall, S.K. Wilson, An alternating direction implicit scheme for parabolic equations with mixed derivative and convective terms, *J. Comput. Phys.* 126 (1) (1996) 64–76.
- [47] A.R. Mitchell, D.F. Griffiths, *The Finite Difference Method in Partial Differential Equations*, Wiley, Chichester, 1980.
- [48] R.K. Mohanty, M.K. Jain, High accuracy difference schemes for the system of two space nonlinear parabolic differential equations with mixed derivatives and variable coefficients, *J. Comput. Appl. Math.* 70 (1) (1996) 15–32.
- [49] K.W. Morton, D.F. Mayers, *Numerical Solution of Partial Differential Equations*, Cambridge University Press, Cambridge, 1994.
- [50] T.G. Myers, Thin films with high surface tension, *SIAM Rev.* 40 (3) (1998) 441–462.
- [51] A. Novick-Cohen, L.A. Segel, Nonlinear aspects of the Cahn–Hilliard equation, *Phys. D* 10 (3) (1984) 277–298.
- [52] A. Oron, Nonlinear dynamics of three-dimensional long-wave Marangoni instability in thin liquid films, *Phys. Fluids* 12 (7) (2000) 1633–1645.
- [53] A. Oron, Three-dimensional nonlinear dynamics of thin liquid films, *Phys. Rev. Lett.* 85 (10) (2000) 2108–2111.
- [54] A. Oron, S.G. Bankoff, Dewetting of a heated surface by an evaporating liquid film under conjoining/disjoining pressures, *J. Coll. Int. Sci.* 218 (1999) 152–166.
- [55] A. Oron, S.H. Davis, S.G. Bankoff, Long-scale evolution of thin liquid films, *Rev. Mod. Phys.* 69 (3) (1997) 931–980.
- [56] R. Peyret, T.D. Taylor, *Computational Methods for Fluid Flow*, Springer, New York, 1983.
- [57] W.H. Press, S.A. Teukolsky, W.T. Vetterling, B.P. Flannery, *Numerical Recipes in C*, 2nd Edition, Cambridge University Press, Cambridge, 1992.
- [58] W.C. Rheinboldt, *Methods for Solving Systems of Nonlinear Equations*, 2nd Edition, SIAM, Philadelphia, PA, 1998.
- [59] L.W. Schwartz, Hysteretic effects in droplet motions on heterogeneous substrates: direct numerical simulation, *Langmuir* 14 (1998) 3440–3453.

- [60] L.W. Schwartz, R.V. Roy, R.E. Eley, S. Petrash, Dewetting patterns in a drying liquid film, *J. Coll. Int. Sci.* 234 (2001) 363–374.
- [61] N.F. Smyth, J.M. Hill, High-order nonlinear diffusion, *IMA J. Appl. Math.* 40 (2) (1988) 73–86.
- [62] J.C. Strikwerda, *Finite Difference Schemes and Partial Differential Equations*, Wadsworth & Brooks/Cole Advanced Books & Software, Pacific Grove, CA, 1989.
- [63] J. Tumblin, G. Turk, LCIS: A boundary hierarchy for detail-preserving contrast reduction, in: *SIGGRAPH '99 Conference Proceedings*, ACM, New York, 1999, pp. 83–90.
- [64] P.J. van der Houwen, B.P. Sommeijer, Approximate factorization for time-dependent partial differential equations, *J. Comput. Appl. Math.* 128 (2001) 447–466.
- [65] G.W. Wei, Generalized Perona-Malik equation for image restoration, *IEEE Sig. Proc. Let.* 6 (7) (1999) 165–167.
- [66] T.P. Witelski, A.J. Bernoff, Dynamics of three-dimensional thin film rupture, *Phys. D* 147 (1–2) (2000) 155–176.
- [67] L. Zhornitskaya, A.L. Bertozzi, Positivity-preserving numerical schemes for lubrication-type equations, *SIAM J. Numer. Anal.* 37 (2) (2000) 523–555.